Human seizures self-terminate across spatial scales via a critical transition

Mark A. Kramer[a,1], Wilson Truccolo[b,c,d,e], Uri T. Eden[a], Kyle Q. Lepage[a], Leigh R. Hochberg[c,d,e,f,g], Emad N. Eskandar[f,h], Joseph R. Madsen[i,j], Jong W. Lee[k], Atul Maheshwari[d,f], Eric Halgren[l], Catherine J. Chu[d,f], and Sydney S. Cash[d,f]

[a]Department of Mathematics and Statistics, Boston University, Boston, MA 02215; [b]Department of Neuroscience, Brown University, Providence, RI 02912; [c]Institute for Brain Science, Brown University, Providence, RI 02912; [d]Department of Neurology, Massachusetts General Hospital, Boston, MA 02114; [e]Rehabilitation Research and Development Service, Department of Veterans Affairs, Providence, RI 02908; [f]Harvard Medical School, Boston, MA 02115; [g]School of Engineering, Brown University, Providence, RI 02912; [h]Department of Neurosurgery and Nayef Al-Rodhan Laboratories for Cellular Neurosurgery and Neurosurgical Technology, Massachusetts General Hospital, Boston, MA 02114; [i]Department of Neurosurgery, Children's Hospital, Boston, MA 02115; [j]Department of Neurosurgery, Brigham and Women's Hospital, Boston, MA 02115; [k]Department of Neurology, Brigham and Women's Hospital, Boston, MA 02115; [l]Departments of Radiology, Neurosciences and Psychiatry, University of California at San Diego, San Diego, CA 92093

Why seizures spontaneously terminate remains an unanswered fundamental question of epileptology. Here we present evidence that seizures self-terminate via a discontinuous critical transition or bifurcation. We show that human brain electrical activity at various spatial scales exhibits common dynamical signatures of an impending critical transition—slowing, increased correlation, and flickering—in the approach to seizure termination. In contrast, prolonged seizures (status epilepticus) repeatedly approach, but do not cross, the critical transition. To support these results, we implement a computational model that demonstrates that alternative stable attractors, representing the ictal and postictal states, emulate the observed dynamics. These results suggest that self-terminating seizures end through a common dynamical mechanism. This description constrains the specific biophysical mechanisms underlying seizure termination, suggests a dynamical understanding of status epilepticus, and demonstrates an accessible system for studying critical transitions in nature.

critical slowing down | epilepsy | electrocorticogram | local field potential

Although extensive observations and research have elucidated some mechanism of seizure initiation and maintenance, how seizures spontaneously terminate remains one of the most important, but still unanswered, questions in epileptology (1). Some of the potential mechanisms of seizure termination (2) include glutamate depletion (3), dynamic changes in ion concentrations (4–6), persistent activation of a hyperpolarization-activated cation conductance (7), changing synaptic effectiveness (5, 8), modulatory effects from subcortical structures and the cerebellum (9), and reduced pH (10). Together, these studies suggest distinct pathways to seizure termination through specific biophysical mechanisms.

We propose here a dynamical understanding of seizure termination that encompasses and constrains these and other hypothesized biophysical mechanisms. Specifically, we propose that focal seizures with secondary generalization terminate in a manner consistent with crossing a critical transition or bifurcation in which the system traverses a critical threshold and shifts suddenly to an alternative, attracting dynamical regime (11). Such regime shifts between alternative stable states have been described in many real-world systems (12–14) and exhibit a repertoire of early warning indicators (15–17). The seizing brain provides a unique living system for studying the signatures of an impending critical transition as well as one in which interventions can have profound practical import.

We characterize the features of seizure termination in both multiscale in vivo data from patients with epilepsy and a computational model of cortical field activity. We show that population electrical activity—observed at macroscopic spatial scales—exhibits numerous signatures of an impending critical transition, whereas spatially localized recordings of neural spiking activity possess different dynamics. These insights offer a generic dynamical understanding of seizure termination emergent in organized neural population activity, with significant implications for understanding status epilepticus and therapeutic advances. Moreover, these observations link seizure termination to critical transitions in diverse natural and synthetic complex systems and demonstrate a biological system for exploring the utility of early warning signals preceding and predicting critical transitions.

Results

Signatures of a Critical Transition in Multiscale Brain Voltage Recordings.
We consider brain electrical activity from multiple spatial scales in patients with different epilepsy etiologies: noninvasive scalp electroencephalogram (EEG) recordings (8 seizures from eight patients), invasive electrocorticogram (ECoG) recordings from the cortical surface (15 seizures from five patients) and deep brain structures (11 seizures from three patients), and local field potential (LFP) recordings and multiunit activity (MUA) from high-density microelectrode arrays implanted in the cortex (10 seizures from three patients) (*Materials and Methods* and SI Appendix, Table S1). In all cases, we selected seizures that began focally and then spread to become generalized (i.e., spread throughout the brain). Voltage recordings during the seizures display well-known stereotypical dynamics (Fig. 1). At all spatial scales, individual electrodes exhibit a characteristic slowing of rhythmic activity during the seizure [i.e., a brain chirp (18)], followed by an abrupt reduction in overall activity apparent through visual inspection of seizure termination (Fig. 1).

To characterize the approach to seizure termination, four early warning measures indicative of an impending critical transition were used: slowing, increased temporal and spatial correlations, and flickering (16). Theory and observations across disciplines suggest that, in the approach to a critical transition, dynamical systems move toward a bifurcation at which the dominant real eigenvalue approaches zero. Therefore, the system recovers more slowly from small perturbations, resulting in slower activity and increased temporal and spatial correlations (13, 14, 19–21). The power spectrum (example for one seizure observed in a surface ECoG recording in Fig. 2A, i) reveals how the activity changes during the seizure: the dominant frequency of the oscillation
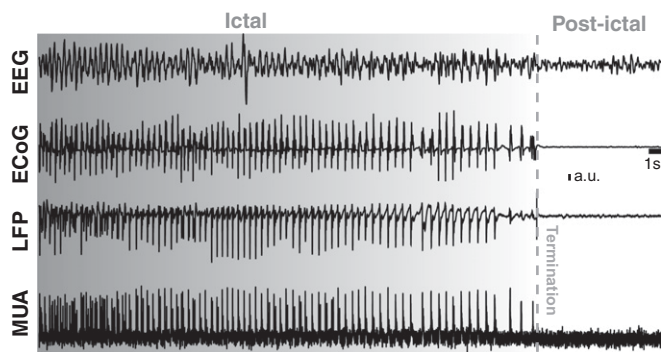
Fig. 1. Brain electrical activity approaching seizure termination observed across spatial scales. Example multiscale voltage traces recorded simultaneously in the scalp EEG, surface ECoG, LFP, and MUA in the approach to seizure termination (vertical dashed line). The abrupt transition from ictal (dark gray) to postictal (white) may exhibit early warning signatures of a critical transition. The activity in each trace has been scaled to permit visual comparison.

decreases as seizure termination approaches. The negative slope of a line fit to the frequency of mean power [i.e., the frequency at which the cumulative power distribution, normalized to unit area, exceeds 0.5 (gray line in Fig. 2*A*, *i*) (*Materials and Methods*)] characterizes this slowing. To assess temporal and spatial correlations within the voltage recordings, we compute the autocorrelation of each time series and the 2D spatial correlation at all spatial scales during the seizure (*Materials and Methods*). We note that the depth ECoG recordings do not possess an appropriate electrode configuration from which to compute a 2D spatial
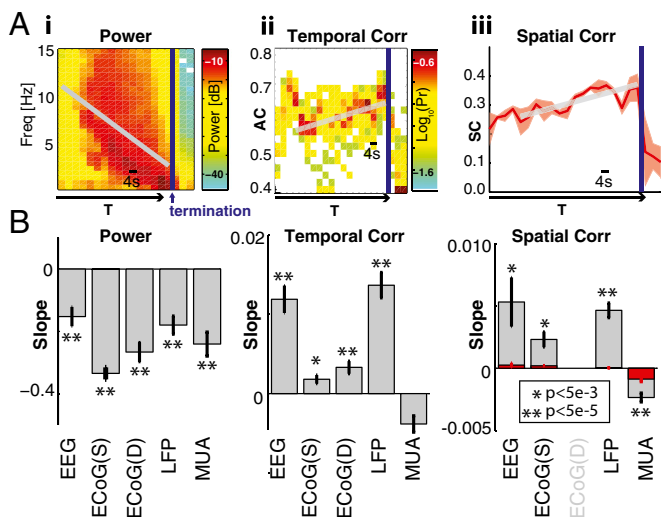

Fig. 2. Critical transition signatures—decreased oscillation frequency and increased correlations—approaching seizure termination. (*A*) Example of power spectrum (*i*), autocorrelation (AC) distribution (*ii*), and 2D spatial correlation (SC, *iii*) of ECoG data versus time (T) in the approach to seizure termination (vertical blue line). To characterize these distributions, a line is fit (gray) to the mean values over time for each measure (*Materials and Methods*). (*B*) Population results for the slope of the linear fits to the frequency of mean power, or mean temporal and spatial correlations, approaching seizure termination. For most measures and spatial scales in EEG, surface ECoG(S), depth ECoG(D), LFP, and MUA, the slopes differ significantly from zero. Black lines indicate the SEM, and asterisks indicate levels of significance; see *P* values in *B* and in text. Spatial correlations are not computed for the ECoG(D) recordings that lack a 2D electrode grid configuration. Red bars indicate the spatial correlations computed for surrogate data.

correlation. Both distributions of correlation values (examples for one surface ECoG recording in Fig. 2 *A*, *ii* and *iii*) increase in the approach to seizure termination. The positive slope of lines fit to the mean correlations over time (gray lines in Fig. 2 *A*, *ii* and *iii*) summarize the results: the electrical activity becomes more temporally and spatially correlated.

Analysis of the population data reveals similar results (Fig. 2*B*). In the approach to seizure termination, the frequency of the mean power decreases at all spatial scales (negative slope, *P* < 5*e*-5 in all cases). For the field potential data, the temporal and spatial correlations increase approaching seizure termination (positive slope, *P* < 5*e*-3), consistent with an impending critical transition. We find similar temporal correlation results for different choices of analysis parameters (*SI Appendix*, Fig. S1). At the smallest spatial scale of observation, the MUA, not all signatures of an impending critical transition appear. The MUA lack a significant change in temporal correlation (*P* = 0.08) and exhibit a significant decrease in spatial correlation (*P* < 5*e*-5) approaching seizure termination.

We might presume that the slowing rhythmic activity during the seizure confounds the correlation analyses. If this were so, we would expect all spatial scales to exhibit similar changes in correlation. However, we find differences in correlation changes across spatial scales, even though all spatial scales exhibit slowing rhythmic activity (Fig. 2*B*). Analysis of Fourier-based surrogate data (22) that preserve the power spectrum of a time series but randomize the phase (*SI Appendix, Analysis and Modeling Methods*) exhibit only weak spatial correlations (Fig. 2*B*, red bars), which suggests that the changing spectral content of the seizure does not produce the changing spatial correlations. In addition, we have analyzed synthetic multivariate time series data consisting of slowing rhythmic activity (starting at 8–12 Hz and ending at 0–1 Hz). In contrast to the in vivo data, these simulations show a reduction in temporal correlations and no change in spatial correlations (*SI Appendix*, Fig. S2). We conclude that the slowing rhythmic activity does not itself produce artifactual changes in the correlation patterns observed in the in vivo voltage data.

Another phenomenon associated with dynamics near a critical transition is "flickering," e.g., when noise pushes a bistable system back and forth between two alternative attractors (16). To assess whether flickering occurs, we compute the variance of the voltage data over small intervals (50 ms) as a simple characterization of the ictal (high variance, Fig. 3*A* in light red) and postictal (low variance, Fig. 3*A* in green) attractor states. Immediately preceding seizure termination, signatures of both attractors appear (example as observed in the surface ECoG data shown in Fig. 3*A*). The variance distribution preceding seizure termination is approximately bimodal (orange in Fig. 3*B*), flickering between the unimodal distributions observed during the ictal period (red in Fig. 3*B*) and the postictal period (green Fig. 3*B*).

To characterize this flickering behavior, we classify the multidimensional variance vector (defined as the variance of each electrode organized as a one-dimensional vector) as belonging to one of three groups: preictal, ictal, or postictal (*SI Appendix, Analysis and Modeling Methods*). Qualitatively, the elements of the variance vectors are large for the ictal group, small for the postictal group, and intermediate for the preictal group, which provides a basic characterization of the dynamic state. To examine the transition to seizure termination, we perform this classification in two periods: (*i*) mid-seizure and (*ii*) just before seizure termination. Within each period, each variance vector is assigned to one of the three groups, and the proportion of variance vectors within each group is determined. Not surprisingly, the ictal group dominates during the mid-seizure period; the large amplitude fluctuations characteristic of seizure produce high variance activity. However, just before seizure termination, this dominance is lost. For the EEG (Fig. 3*C*) and ECoG data (Fig. 3 *D* and *E*), the proportion of vectors classified as ictal (red)
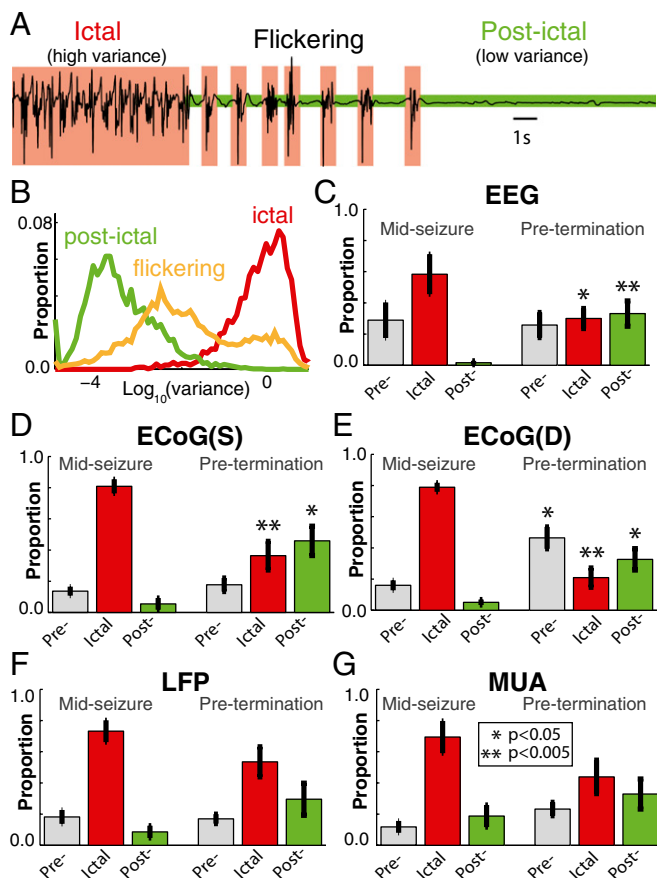
Fig. 3. Multiscale voltage data flicker between ictal and postictal states approaching seizure termination. (*A*) Example of flickering in ECoG data preceding seizure termination. Between the ictal (light red) and postictal (green) states, signatures of both states appear. (*B*) Proportion of signal variance during ictal (red), flickering (orange), and postictal (green) intervals. The flickering interval exhibits a broad variance distribution with two peaks. (*C–G*) The proportion of variance vectors classified as preictal (gray), ictal (red), and postictal (green) in two periods: mid-seizure and pretermination. For the EEG (*C*), surface ECoG (*D*), and depth ECoG (*E*), the changes in classification from ictal to postictal are significant. For the LFP (*F*) and MUA (*G*), similar trends exists but are not significant.

significantly decreases (EEG: $P = 0.018$; ECoG: $P < 5e$-4), whereas the proportion of vectors classified as postictal (green) significantly increases (EEG: $P = 0.003$; ECoG: $P < 5e$-3) preceding seizure termination. A similar trend appears in the LFP (Fig. 3*F*) and MUA (Fig. 3*G*) data, although the changes in the classifications are not significant ($P > 0.1$ in all cases). In most cases, the proportion of vectors classified as preictal (gray in Fig. 3) does not significantly change ($P > 0.1$ for all cases except depth ECoG in which $P = 0.012$). These empirical observations support premonitory flickering between two dynamical states— the ictal and postictal attractors—in the approach to seizure termination.

Fig. 4 summarizes the critical transition indicators computed at each spatial scale. Recordings at macroscopic spatial scales (EEG and ECoG) display signatures of an impending critical transition approaching seizure termination; note that spatial correlations cannot be meaningfully computed for the depth ECoG recordings. At the smaller spatial scales, the LFP data exhibit three of the four computed indicators [and a trend toward flickering behavior (Fig. 3*F*)]. However, observations of MUA display only one of the four indicators—slowing rhythmic activity, as observed across all spatial scales (first row in Fig. 4); additional analyses based on the

neuronal spike counts across the ensemble of sorted single units led to similar results (*SI Appendix*, Figs. S3–S5). We conclude that the neural field activity, but not the multiunit activity or the single-unit population spike count, display clear characteristic warning signs of an impending critical transition in the approach to seizure termination.

Signatures of a Critical Transition in a Mean-Field Model of Seizure Termination. To further investigate the proposed critical transition at seizure termination, we implement a mean-field model of cortical activity. Rather than representing the electrical activity of an individual neuron, mean-field or "lumped" models represent the aggregate activity of neural populations and are therefore particularly suitable for representing neural fields—such as the EEG, ECoG, and LFP of primary interest here—which are thought to represent the coordinated synaptic and intrinsic currents of neural populations (23–25). Mean-field models have a long history in computational neuroscience (e.g., 26–29), including many important applications for seizure modeling. These include, for example, mean-field models of absence seizures (30–32), of depth and surface electrode recordings from patients with temporal lobe epilepsy (33, 34), seizure generalization (35), and anesthetic-induced seizures (36).

Here the model variables (*SI Appendix*, Eq. **S1**) correspond to the average excitatory and inhibitory activity of neural populations and their synaptic interactions, representative of the field potentials observed (37). For a single mean-field oscillator, adjusting a parameter representative of excitatory synaptic strength results in a critical transition (Fig. 5*A*), specifically a fold bifurcation of limit cycles (Fig. 5*C*). Qualitatively, as the connectivity strength increases, the dynamics shift from large-amplitude ictal oscillations (Fig. 5*A, i*) to small-amplitude postictal fluctuations (Fig. 5*A, iii*). Immediately preceding this shift is a region of bistability that flickers between both types of dynamics (Fig. 5*A, ii*); in this case, noise pushes the system between the two attractor states. These changes correspond to the transition from a branch of attracting limit cycles to a branch of attracting fixed points, which is preceded by a region of bistability between the two attractors separated by a branch of repelling limit cycles born in a subcritical Hopf bifurcation (Fig. 5*C*). Simulations from a population of stochastic mean-field oscillators [64 columns arranged in an 8-×-8 grid with nearest neighbor excitatory synapses and periodic boundary conditions (*SI Appendix, Analysis and Modeling Methods*)] show rhythmic and correlation changes consistent with the brain voltage data: the oscillation frequency decreases, whereas the temporal and spatial correlations increase in the approach to seizure termination (Fig. 5*B* and *SI Appendix*, Fig. S6). In addition, just before the critical transition there exists a region of flickering, characterized by intervals of variance consistent with the ictal (high variance) and the postictal (low variance) states (Fig. 5*D*).

These results support the conclusion that a generic mechanism— a discontinuous critical transition—underlies seizure termination, here implemented through a specific dynamical mechanism (a fold of limit cycles) and biophysical mechanism (strengthened

	EEG	ECoG (S)	ECoG (D)	LFP	MUA
Slowing rhythms	**YES**	**YES**	**YES**	**YES**	**YES**
Increased **temporal** correlations	**YES**	**YES**	**YES**	**YES**	NO
Increased **spatial** correlations	**YES**	**YES**	—	**YES**	NO
Flickering	**YES**	**YES**	**YES**	NO	NO

Fig. 4. Summary of critical transition signatures determined at each spatial scale. The scalp EEG and ECoG data (shaded in gray) display all four warning signs of an impending critical transition approaching seizure termination. Spatial correlations are not meaningful for the depth ECoG [i.e., ECoG (D)] recordings. The MUA exhibit only slowing rhythmic activity, as observed across all spatial scales in the approach to seizure termination.
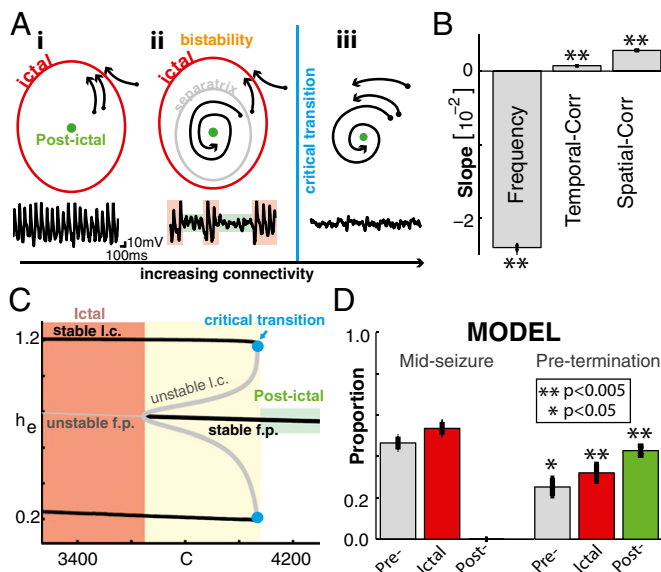
Fig. 5. Computational model of seizure termination mimics the observed dynamics. (*A*) Cartoon illustration of the transition from ictal to postictal in the mean-field model. At low connection strength (*A, i*), all dynamics (black) approach the ictal attractor (red). Bistability precedes the discontinuous critical transition (*A, ii*); dynamics outside the separatrix (gray) approach the ictal attractor, and dynamics inside the separatrix approach the postictal attractor (green). After the critical transition (*A, iii*), only the postictal attractor remains. (*Lower*) Simulated voltage traces illustrate the model dynamics in each case. During the interval of bistability (*A, ii*), flickering occurs between the ictal (red shading) and postictal (green shading) states. (*B*) Fits to the slope of the frequency of mean power, mean temporal correlations, and mean spatial correlations for a population of field oscillators as connectivity strength increases. In all cases, the values differ significantly from zero. Surrogate data do not yield notable spatial correlations in the model. (*C*) Bifurcation diagram of the self-connected mean-field model (*SI Appendix, Mean Field Model*) reveals a region of bistability. One model variable, the main observable h_e, is plotted versus the bifurcation parameter *C*, the connection strength. At weaker connection strengths, the only attractor consists of stable limit cycles (l.c.), which correspond to large-amplitude oscillations characteristic of the ictal state (shaded light red). Increased connection strength ("C" on the *x* axis) induces bistability (yellow interval) in which another attractor appears, a branch of stable fixed points (f.p.). At the critical transition (blue circles) the bistability is lost and the only stable attractor becomes the branch of fixed points (shaded green). (*D*) Proportion of variance vectors classified as preictal (gray), ictal (red), and postictal (green) in an intermediate-connectivity (mid-seizure) and high-connectivity (pre-termination) state for the population of mean-field oscillators. Flickering manifests in the pre-termination interval as significant changes in the proportions of ictal and postictal classifications.

excitatory synapses). This biophysical mechanism is consistent with an increase in long-range spatial correlations in brain electrical activity, perhaps reflecting a self-organizing process for seizure termination that drives large neuronal networks into a hypo-excitable state (1, 8). In this case, an activity-dependent process (i.e., the excitatory synaptic strength changing as a function of neural activity) leads to seizure termination. Important model extensions would incorporate realistic activity-dependent processes directly into the dynamics (38) to systematically explore the biophysical mechanisms of seizure termination. Although the model mimics the dynamics of seizure termination, the specific mechanism in this model is not unique; we propose that other pathways are possible (Fig. 6) involving different bifurcations (39) and biophysical mechanisms consistent with the generic dynamical principle of a critical transition. Moreover, different seizure types may involve different biological and dynamical mechanisms, for example, the role of a hyperpolarization-activated cation conductance (7) in terminating

generalized absence seizures as simulated through activity-dependent transitions in a bistable neural model (38). Refining a general dynamical understanding at the macroscopic spatial scale to specific biophysical and dynamical processes governing seizure termination at the microscopic spatial scale remains a crucial issue and will require both detailed computational models (6, 40) and experiments (41).

Status Epilepticus: Failure to Cross the Critical Transition. Status epilepticus—when a seizure fails to spontaneously self-terminate—is a life-threatening condition requiring immediate medical attention. To understand the dynamical mechanisms of status epilepticus, we consider the mean-field model used above to characterize seizures with spontaneous self-termination (Fig. 5). In this model, a seizure fails to self-terminate if it approaches the critical transition, but does not cross it and instead retreats back to the ictal attractor (Fig. 7*A*). Approaching and retreating from the critical transition produces characteristic dynamical traits in the mean-field model: approaching the critical transition, the frequency of mean power decreases and the autocorrelation increases (Fig. 5*B*), as observed for self-terminating seizures (examples in Fig. 7*B*); retreating from the critical transition produces an opposite effect (i.e., an increase in the frequency of mean power and a decrease in the autocorrelation). These model results motivate the hypothesis that voltage recordings from the human brain during status epilepticus exhibit similar behaviors. To test this, we analyzed 600 s of scalp EEG ($n = 4$) and surface ECoG ($n = 1$) data during status epilepticus (*SI Appendix, Patient Information* and *Analysis and Modeling Methods*). The model and in vivo data exhibit qualitatively similar changes in the frequency of mean power and mean autocorrelation (example in Fig. 7*C*). To characterize the association between these two measures, we compute their cross-correlation; the cross-correlation is negative at zero lag (illustrated in Fig. 7*D* as one example) both for the patients with status epileptics and for the patients with self-terminating seizures (Fig. 7*E*). However, all patients with status epilepticus exhibit periodicity at positive and negative lags (example in Fig. 7*D* and in *SI Appendix, Fig. S7*) in the cross-correlation, indicating repeatability of the behavior not observed in self-terminating seizures. Analysis of synthetic data simulating repeated intervals of reduced frequency of mean power produce a strong positive correlation between the two measures, which suggests that the in vivo results are not an artifact of the analysis (*SI Appendix, Fig. S7*). We propose that during status epilepticus the system repeatedly approaches the critical transition, but never quite reaches it, and instead retreats to the ictal attractor. In this case, the seizure fails to spontaneously
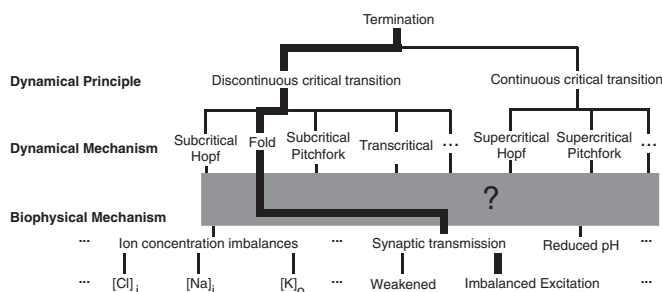

Fig. 6. Outline of potential seizure termination scenarios. The solid black line highlights the computational model implemented here, in which the critical transition (*Top*) is implemented through a specific dynamical mechanism (examples in the *Middle*) and biophysical mechanism (examples at the *Bottom*). Many prospective biophysical mechanisms exist, each potentially associated with multiple types of dynamical mechanisms or even principles at the macroscopic spatial scale and perhaps with different dynamical mechanisms at the microscopic spatial scale.
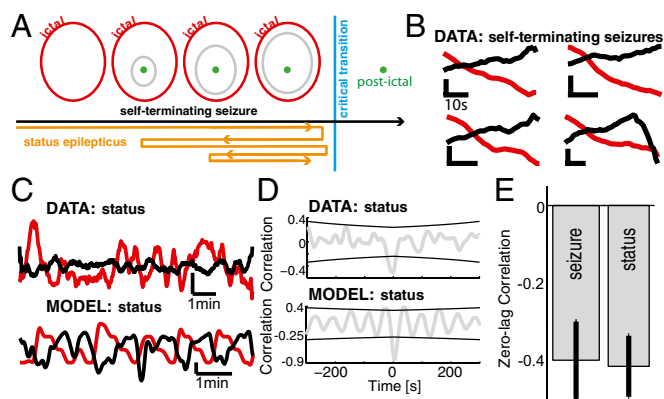
Fig. 7. Status epilepticus represents failure to cross the seizure critical transition. (*A*) Cartoon illustration of status epilepticus dynamics. As a self-terminating seizure progresses from ictal attractor to postictal attractor (solid black line, as in Fig. 5), the separatrix (gray ellipse) enlarges, eventually colliding with the ictal attractor (red ellipse) at the critical transition. In status epilepticus, the system approaches the critical transition but repeatedly retreats toward regions that support the ictal attractor (orange lines). (*B* and *C*) Examples of frequency of mean power (red) and mean autocorrelation (black) for four self-terminating seizures (*B*), during status epilepticus (*C*, *Upper*), and in the model (*C*, *Lower*). The self-terminating seizures are brief compared with status epilepticus. In all cases, visual inspection suggests anticorrelation between the two measures. Vertical scale bars indicate SD from the mean. (*D*) The cross-correlation (gray) between the two measures for the clinical and simulated status epilepticus data in *C* reveals anticorrelation at zero lag and rhythmicity. The black curves indicate 1.5 times the expected SD computed using the Bartlett estimator (42). (*E*) The cross-correlation at zero lag for patients with status epilepticus (*n* = 5, label "status"; mean: −0.41, SEM 0.07) and scalp EEG and surface ECoG data for self-limited seizures (*n* = 23, label "seizure"; mean: −0.40, SEM 0.1) is negative.

self-terminate and the repeated approach and retreat from the critical transition continues until another intervention (e.g., drug delivery) is provided.

Discussion

Existing models of brain activity use attractor bistability (or multistability) both for normal function [e.g., memory (43–45)] and critical transitions or phase transitions for biological coordination (13). Seizures have often been conceptualized as a single attractor state alternative to normal brain activity (32, 46). Although signatures of a critical transition at seizure onset have been proposed (47), experimental evidence directly supporting the existence of bistability between an ictal attractor and postictal attractor is lacking. Here we focus on termination of focal seizures with secondary generalization—an easily identified and stereotyped brain transition—to propose that the ictal-to-postictal change occurs in a discontinuous critical transition between two alternate attractor states. Although conclusive identification of a catastrophic bifurcation from time series data remains infeasible (14), the dynamic signatures and model all support the hypothesis that seizures spontaneously self-terminate through a critical transition at multiple macroscopic spatial scales.

The mean-field model used here (constructed to mimic the electrical activity during seizure) motivated a specific dynamical hypothesis: that status epilepticus could be understood as a repeated approach and retreat from a critical transition. Such behavior exhibits dynamical characteristics that can be tested in vivo. We have done so and found for each patient evidence consistent with this dynamical hypothesis. We note that status epilepticus is a complicated and evolving brain state and that the entire event exhibits changing dynamical properties (e.g., due to intrinsic brain mechanisms and, typically, pharmacological interventions). However, each patient exhibited a long interval (10 min) of dynamic

activity consistent with the model prediction. These results provide an initial dynamical characterization of status epilepticus. We propose that status epilepticus results from the failure of an underlying brain mechanism to drive the system through the critical transition. This may occur due to alternative mechanisms acting against spontaneous termination or to a pathology in the usual self-termination mechanism. In either case, dynamical treatment strategies (e.g., targeted interventions designed to push the system past the critical transition at the point of closest approach) can be explored.

Seizure activity appears across all spatial scales of the human brain—from the individual neuron (48) to the scalp surface. The analysis presented here suggests that a critical transition occurs at seizure termination in neural field activity, as observed in the EEG, ECoG, and LFP. Despite clear and abrupt suppression of neuronal spiking during seizure termination (48), consistent signatures of an impending critical transition at seizure termination were not detected at the level of MUA or population spiking based on sorted single units. More robust precursor signatures of a critical transition may perhaps occur in different spatially focal locations not observed. Alternatively, the seizure may represent a macroscopic brain phenomenon, requiring the collective cooperation of neural populations for maintenance and eventually termination. We note that the specific dynamical mechanisms at the microscopic spatial scale (e.g., the bifurcation from rest to spiking in a single neuron) may differ from the critical transition observed at the macroscopic spatial scale during seizure. In this case, precursor signatures of a critical transition at the macroscopic spatial scale are an emergent phenomenon depending on a population of neurons and thus would not be apparent in the individual neuron dynamics, but would still be dependent on the coordination of biophysical mechanisms at the microscopic spatial scale.

The hypothesis of a critical transition at seizure termination links the potentially diverse biophysical mechanisms of the seizures analyzed here (focal seizures with secondary generalization) under a common dynamical framework. This is analogous to the idea that multiple genetic and epigenetic factors can contribute to produce the same epileptic state (23). Although seizure termination occurs through a variety of biophysical routes, we propose that all of these routes follow a common dynamical pathway. This generic dynamical mechanism constrains computational models of this seizure type to exhibit specific dynamical characteristics at termination in the macroscopic field activity and suggests two immediate experimental predictions: coexistence of alternative attractors and hysteresis. First, immediately preceding seizure termination, alternative stable attractors, representing the ictal and postictal states, coexist. Second, a seizing system driven in reverse from the postictal to ictal state will exhibit hysteresis, so that the postictal state remains stabilized even as the system's conditions return past the critical transition. Both features are present in the computational model, and empirical evidence supports the existence of alternative attractors. However, definitive tests of these predictions will require optimized techniques to characterize the ictal and postictal states (beyond a simple measure of variance) and detailed in vitro experiments that allow precise control of biophysical manipulations. We note that different seizure types exhibit different voltage characteristics (e.g., the sudden onset and termination of absence seizures) whose biophysical and dynamical mechanisms likely differ from those proposed here.

Critical transitions or "tipping points" provide a common dynamical understanding linking diverse phenomena from natural and synthetic complex systems (14). Detecting generic indicators of an impending critical transition has broad implications for management of disease (49), ecosystems (19, 50), financial markets (16), and the Earth's climate (15, 51). In particular, knowledge of an impending critical transition can permit intervention to promote a preferred state (e.g., biomanipulation in ecosystems). However, real-world tests of these indicators and manipulations are typically rare, expensive, and difficult to repeat. Unlike other

complex systems (e.g., the climate), neural dynamics possess both detailed computational models and manageable experimental systems in which transitions occur over minutes rather than days (17), years (50), or centuries (15). For seizures, understanding and manipulating the biophysical processes that promote the critical transition—by decreasing the resilience of the ictal state or by increasing the resilience of the postictal state—may suggest anticonvulsant or device-based therapies focused on treating the disease dynamics. Further study will have implications for both epilepsy therapy and the development of theoretical approaches to understanding and predicting critical transitions in the natural world.

Materials and Methods

Patients with medically intractable focal epilepsy were considered. EEG data were recorded using a standard 10–20 electrode configuration from eight patients (two female, age 40 ± 11 y). ECoG data were recorded using standard recording systems (XLTEK) from eight patients (three female, age 33 ± 10 y). For five patients, an 8-by-8 electrode array (1-cm spacing) was used. For three patients, depth electrodes (1-cm spacing) sampled mesial structures. LFP data, MUA, and single-unit activity were recorded from three patients using 96 microelectrode arrays covering a 4×4-mm patch of

neocortex (one female, ages 21, 32, and 52 y). Seizure onset and termination times were determined by an experienced encephalographer (S.S.C.). Electrode implantation decisions were made entirely on clinical grounds without reference to this project. Five patients with status epilepticus were considered (four EEG recordings, three females, age 43 ± 20 y; one ECoG recording, male, age 24 y). Research approval was granted by local Institutional Review Boards (Partners Human Research Committee and Boston University), and patients were enrolled after informed consent was obtained. Detailed discussion of the clinical recordings, microelectrode array recordings (48), data preprocessing, single subject and population analysis, computational modeling, and statistical analysis may be found in SI Appendix.

1. Schindler K, Elger CE, Lehnertz K (2007) Increasing synchronization may promote seizure termination: Evidence from status epilepticus. *Clin Neurophysiol* 118(9): 1955–1968.
2. Lado FA, Moshé SL (2008) How do seizures stop? *Epilepsia* 49(10):1651–1664.
3. Kullmann DM, Semyanov A (2002) Glutamatergic modulation of GABAergic signaling among hippocampal interneurons: Novel mechanisms regulating hippocampal excitability. *Epilepsia* 43(Suppl 5):174–178.
4. Bragin A, Penttonen M, Buzsáki G (1997) Termination of epileptic afterdischarge in the hippocampus. *J Neurosci* 17(7):2567–2579.
5. Fröhlich F, Bazhenov M, Timofeev I, Sejnowski TJ (2005) Maintenance and termination of neocortical oscillations by dynamic modulation of intrinsic and synaptic excitability. *Thalamus Relat Syst* 3(2):147–156.
6. Krishnan GP, Bazhenov M (2011) Ionic dynamics mediate spontaneous termination of seizures and postictal depression state. *J Neurosci* 31(24):8870–8882.
7. Bal T, McCormick DA (1996) What stops synchronized thalamocortical oscillations? *Neuron* 17(2):297–308.
8. Timofeev I, Steriade M (2004) Neocortical seizures: Initiation, development and cessation. *Neuroscience* 123(2):299–336.
9. Norden AD, Blumenfeld H (2002) The role of subcortical structures in human epilepsy. *Epilepsy Behav* 3(3):219–231.
10. Ziemann AE, et al. (2008) Seizure termination by acidosis depends on ASIC1a. *Nat Neurosci* 11(7):816–822.
11. Strogatz S (2001) *Nonlinear Dynamics And Chaos* (Westview Press, Boulder, CO).
12. Haken H (1983) *Synergetics, an Introduction: Nonequilibrium Phase Transitions and Self-Organization in Physics, Chemistry, and Biology* (Springer-Verlag, New York).
13. Kelso JAS (1995) *Dynamic Patterns: The Self-Organization of Brain and Behavior* (MIT Press, Cambridge, MA).
14. Scheffer M (2009) *Critical Transitions in Nature and Society* (Princeton Univ Press, Princeton, NJ).
15. Dakos V, et al. (2008) Slowing down as an early warning signal for abrupt climate change. *Proc Natl Acad Sci USA* 105(38):14308–14312.
16. Scheffer M, et al. (2009) Early-warning signals for critical transitions. *Nature* 461 (7260):53–59.
17. Drake JM, Griffen BD (2010) Early warning signals of extinction in deteriorating environments. *Nature* 467(7314):456–459.
18. Schiff SJ, et al. (2000) Brain chirps: Spectrographic signatures of epileptic seizures. *Clin Neurophysiol* 111(6):953–958.
19. Rietkerk M, Dekker SC, de Ruiter PC, van de Koppel J (2004) Self-organized patchiness and catastrophic shifts in ecosystems. *Science* 305(5692):1926–1929.
20. Dakos V, van Nes E, Donangelo R, Fort H, Scheffer M (2010) Spatial correlation as leading indicator of catastrophic shifts. *Theor Ecol* 3(3):163–174.
21. Veraart AJ, et al. (2012) Recovery rates reflect distance to a tipping point in a living system. *Nature* 481(7381):357–359, 10.1038/nature10723.
22. Schreiber T, Schmitz A (2000) Surrogate time series. *Physica D* 142:346–382.
23. Lytton WW (2008) Computer modelling of epilepsy. *Nat Rev Neurosci* 9(8):626–637.
24. Deco G, Jirsa VK, Robinson PA, Breakspear M, Friston K (2008) The dynamic brain: From spiking neurons to neural masses and cortical fields. *PLOS Comput Biol* 4(8): e1000092.
25. Buzsáki G, Anastassiou CA, Koch C (2012) The origin of extracellular fields and currents: EEG, ECoG, LFP and spikes. *Nat Rev Neurosci* 13(6):407–420, 10.1038/nrn3241.
26. Wilson HR, Cowan JD (1972) Excitatory and inhibitory interactions in localized populations of model neurons. *Biophys J* 12(1):1–24.
27. da Silva FHL, Hoeks A, Smits H, Zetterberg L (1974) Model of brain rhythmic activity. *Biol Cybern* 15(1):27–37.
28. Nunez PL (1974) The brain wave equation: A model for the EEG. *Math Biosci* 21(3–4): 279–297.
29. Freeman WJ (1978) Models of the dynamics of neural populations. *Electroencephalogr Clin Neurophysiol Suppl*, 1978(34)9–18.
30. Lopes da Silva FH, et al. (2003) Dynamical diseases of brain systems: Different routes to epileptic seizures. *IEEE Trans Biomed Eng* 50(5):540–548.
31. Bouwman BM, Suffczynski P, Lopes da Silva FH, Maris E, van Rijn CM (2007) GABAergic mechanisms in absence epilepsy: A computational model of absence epilepsy simulating spike and wave discharges after vigabatrin in WAG/Rij rats. *Eur J Neurosci* 25(9):2783–2790.
32. Breakspear M, et al. (2006) A unifying explanation of primary generalized seizures through nonlinear brain modeling and bifurcation analysis. *Cereb Cortex* 16(9): 1296–1313.
33. Wendling F, Bellanger JJ, Bartolomei F, Chauvel P (2000) Relevance of nonlinear lumped-parameter models in the analysis of depth-EEG epileptic signals. *Biol Cybern* 83(4):367–378.
34. Kramer MA, Kirsch HE, Szeri AJ (2005) Pathological pattern formation and cortical propagation of epileptic seizures. *J R Soc Interface* 2(2):113–127.
35. Kim JW, Roberts JA, Robinson PA (2009) Dynamics of epileptic seizures: Evolution, spreading, and suppression. *J Theor Biol* 257(4):527–532.
36. Wilson MT, Sleigh JW, Steyn-Ross DA, Steyn-Ross ML (2006) General anesthetic-induced seizures can be explained by a mean-field model of cortical dynamics. *Anesthesiology* 104(3):588–593.
37. Liley DTJ, Cadusch PJ, Dafilis MP (2002) A spatially continuous mean field theory of electrocortical activity. *Network* 13(1):67–113.
38. Koppert MMJ, Kalitzin S, Lopes da Silva FH, Viergever MA (2011) Plasticity-modulated seizure dynamics for seizure termination in realistic neuronal models. *J Neural Eng* 8(4):046027.
39. Kuehn C (2011) A mathematical framework for critical transitions: Bifurcations, fast–slow systems and stochastic dynamics. *Physica D* 240(12):1020–1035.
40. Traub RD, et al. (2005) Single-column thalamocortical network model exhibiting gamma oscillations, sleep spindles, and epileptogenic bursts. *J Neurophysiol* 93(4): 2194–2232.
41. McCormick DA, Contreras D (2001) On the cellular and network bases of epileptic seizures. *Annu Rev Physiol* 63:815–846.
42. Netoff TI, Schiff SJ (2002) Decreased neuronal synchronization during experimental seizures. *J Neurosci* 22(16):7297–7307.
43. Durstewitz D, Seamans JK, Sejnowski TJ (2000) Neurocomputational models of working memory. *Nat Neurosci* 3(Suppl):1184–1191.
44. Hopfield JJ (1982) Neural networks and physical systems with emergent collective computational abilities. *Proc Natl Acad Sci USA* 79(8):2554–2558.
45. Lisman JE, Fellous JM, Wang XJ (1998) A role for NMDA-receptor channels in working memory. *Nat Neurosci* 1(4):273–275.
46. da Silva FL, et al. (2003) Epilepsies as dynamical diseases of brain systems: Basic models of the transition between normal and epileptic activity. *Epilepsia* 44(Suppl 12):72–83.
47. McSharry PE, Smith LA, Tarassenko L (2003) Prediction of epileptic seizures: Are nonlinear methods relevant? *Nat Med* 9(3):241–242; author reply, 242.
48. Truccolo W, et al. (2011) Single-neuron dynamics in human focal epilepsy. *Nat Neurosci* 14(5):635–641, 10.1038/nn.2782.
49. Venegas JG, et al. (2005) Self-organized patchiness in asthma as a prelude to catastrophic shifts. *Nature* 434(7034):777–782.
50. Carpenter SR, et al. (2011) Early warnings of regime shifts: A whole-ecosystem experiment. *Science* 332(6033):1079–1082.
51. Lenton TM, et al. (2008) Tipping elements in the Earth's climate system. *Proc Natl Acad Sci USA* 105(6):1786–1793.

NEUROSCIENCE